


Half-lives of deformed nuclei for exotic cluster decays

S. S. Hosseini and S. M. Motevalli*

Department of Physics, Faculty of Science, University of Mazandaran, P.O. Box 47415-416, Babolsar, Iran (Received 3 December 2022; revised 24 February 2023; accepted 3 March 2023; published 21 March 2023)

In this paper, we considered the cluster radioactivity half-lives for all known cluster decay modes (i.e., from ^{14}C up to ^{34}Si) that these nuclei were first satisfied by the observed systematics [Silisteanu and Scheid, *Phys. Rev. C* **51**, 2023 (1995), Poenaru *et al.*, *Phys. Rev. C* **83**, 014601 (2011); Ni *et al.*, *Phys. Rev. C* **78**, 044310 (2008)]. The Coulomb and proximity potential model for deformed nuclei is considered as penetration of the emitter particle through the potential barrier formed by the nuclear, Coulomb, and centrifugal interactions between the emitter particle and nucleus. The spins and parities of the parent and daughter nuclei in addition to the quadrupole (β_2) and hexadecapole (β_4) deformations of the parent nuclei are taken into account for the calculation of the cluster radioactivity half-lives. Our results exhibit, which the minimum $\log_{10}T_{1/2}$ value denotes doubly magic ^{208}Pb ($Z = 82$, $N = 126$) as the daughter nuclei.

DOI: [10.1103/PhysRevC.107.034611](https://doi.org/10.1103/PhysRevC.107.034611)**I. INTRODUCTION**

Cluster radioactivity (CR) by heavy nuclei with an emitted cluster (EC) heavier like carbon and oxygen is heavier than an alpha particle but lighter than fission fragments, which was theoretically proposed in 1980 by Sandulescu, Poenaru, and Greiner [1]. In 1984, Rose and Jones [2] observed the emission of ^{14}C (carbon) nucleus by ^{223}Ra . Since then, other cluster radioactivity has been observed leading to ^{20}O (oxygen) radioactivity, ^{23}F (fluorine) radioactivity, $^{22,24-46}\text{Ne}$ (neon) radioactivity, $^{28,30}\text{Mg}$ (magnesium) radioactivity, and $^{32,34}\text{Si}$ (silicon) emission, and calculated their partial half-lives. In recent years, many theoretical models have been published to estimate the half-lives for the exotic decay procedures [3–10]. Several theoretical models have been used to describe the cluster radioactivity phenomenon. These models may generally be characterized into the preformed cluster model (PCM) [11] in which the cluster is preformation within the parent nucleus [12,13] (like that of Gupta and collaborators based on collective potential energy surfaces) and the superasymmetric fission model (SAFM) [3] (or the analytic superasymmetric fission model (ASAFM) [14]) in which the parent nucleus is assumed to be deformed continuously as it penetrates the nuclear barrier and the cluster is formed like a fission fragment. Poenaru *et al.* [14] considered the cluster radioactivity, alpha decay, and fission for Ne, Mg, and Si. The radioactive decay of heavy nuclei ^{232}Th , ^{236}U , ^{236}Pu , and ^{242}Cm was studied by Tretyakova [15]. The CR processes using the preformed cluster model (PCM) approach were evaluated by Refs. [16,17]. Zhongzhou *et al.* [18] investigated the experimental data of cluster radioactivity and expressed an empirical formula. Poenaru *et al.* [19] calculated the half-lives of spontaneous emission of C, O, F, Ne, Mg, and Si. Based on

inclusion or noninclusion of the concept of cluster preformation probability P_0 , the exotic CRs are generally classified [14] as the preformed cluster models (PCMs) (where $P_0 \neq 1$) and the unified fission models (UFMs) ($P_0 = 1$). Also, a method extensively used in nuclear cluster physics is the local potential model (LPM), as introduced originally by Buck *et al.*, [20]. Souza *et al.*, [21] investigated the $\alpha + \text{core}$ properties of ^{104}Te along with a global discussion on the α -cluster structure above the double-shell closures based on the LPM. In this process, the nucleus is supposed to be a cluster + core system where the two components interact through a deep local phenomenological potential $V(r)$ containing the nuclear and Coulomb terms where $\alpha + \text{core}$ interaction is defined by the local potential, $V(r) = V_C(r) + V_N(r)$. Detailed information about the LPM can be found in papers [22–25]. Many other suitable studies have also been expanded, such as Refs. [26–31], but will not be further propounded in this paper. In the present paper, we consider the decay of radioactive nuclei which emit heavy clusters such as C, O, Ne, Mg, and Si within the Coulomb and proximity potential model for deformed nuclei (CPPMDN).

This paper is organized as follows. The theoretical model used for the study of the CR is presented in Sec. II. In Sec. III, the cluster radioactivity half-lives have been calculated by using the semiempirical formula. The results and discussions are involved in Sec. IV. A summary is given in Sec. V.

II. DETAILS OF THE MODEL WITH PROXIMITY 1977 (PROX 77)

In the present model, for exotic cluster decays, the EC is supposed to be spherical but the parent and daughter nuclei may have axially been a symmetric deformation where θ is the polar angle between the axis of symmetry of the parent or daughter and the direction of EC. The decay half-life $T_{1/2}$ is

* motavali@umz.ac.ir

defined as [32,33]

$$T_{1/2} = \frac{\ln 2}{\lambda} = \frac{\ln 2}{\nu P} = \frac{h \ln 2}{2 E_v P}, \quad (1)$$

where P is the quantum penetrability of the barrier, $\nu = \omega/2\pi$, is the frequency of collision with the barrier per second and “ h ” is the Planck constant, and $E_v = h\nu/2$ is the zero-point vibration energy. We know that the electron charge $e = 1.43998$ MeV fm. The other numerical constants are given by $h \ln 2/2 = 1.4333 \times 10^{-21}$ MeV s and $2\sqrt{2m}/\hbar = 2\sqrt{2}/\sqrt{41.47}$ MeV $^{-1/2}$ fm $^{-1} = 0.43921$ MeV $^{-1/2}$ fm $^{-1/2}$ and $\hbar^2/m = 41.47$ MeV fm 2 where m is the nucleon mass. Using a one-dimensional Wentzel-Kramers-Brillouin (WKB) approximation, the penetration probability is given as

$$P = \exp\left(\frac{-2}{\hbar} \int_{R_a}^{R_b} \sqrt{2\mu [V(\bar{r}) - Q]} dr\right), \quad (2)$$

where R_a and R_b are the turning points and Q is the decay energy expressed in MeV. The Q value in Eq. (2) is the energy released as carrying the shell correction part only as the value at the touching point in the cluster decay process. The turning boundaries are calculated via $V_\ell(R_a) = V_\ell(R_b) = Q$. Also, μ in the above equation is the reduced mass of the cluster-core (daughter) system measured in units of the nucleon mass, i.e., $\mu = mA_d A_c / (A_d + A_c)$, where m is the nucleonic mass measured in units of MeV/ c^2 and A_d and A_c denote the mass numbers of daughter and emitted cluster, respectively. We must notice that, in this paper, we approximate nuclear inertia with the reduced mass [13]. Within CPPMDN, the potential energy barrier is considered as a sum of the Coulomb $V_C(r)$, nuclear proximity $V_N(r)$, and centrifugal $V_\ell(r)$ potentials for the touching configuration and the separated fragments. The potential $V(r)$ is made up of two parts in the overlapping ($\bar{r} < \bar{C}_t$) and nonoverlapping ($\bar{r} \geq \bar{C}_t$) regions [34,35], which is given by

$$V(\bar{r}) = \begin{cases} a_0 + a_1 \bar{r} + a_2 \bar{r}^2, & \text{for } \bar{R}_p \leq \bar{r} \leq \bar{C}_t \\ V_C(\bar{r}) + V_{\text{prox}}(z) + V_\ell(\bar{r}), & \text{for } \bar{r} \geq \bar{C}_t \end{cases}, \quad (3a)$$

$$V_C(\bar{r}) = \begin{cases} a_0 + a_1 \bar{r} + a_2 \bar{r}^2, & \text{for } \bar{R}_p \leq \bar{r} \leq \bar{C}_t \\ V_C(\bar{r}) + V_{\text{prox}}(z) + V_\ell(\bar{r}), & \text{for } \bar{r} \geq \bar{C}_t \end{cases}, \quad (3b)$$

where a_0, a_1, a_2 are the constants determined from the continuity conditions of the potential and its derivative equations, $V(\bar{R}_p) = Q$, $V(\bar{r}) = V(\bar{C}_t)$, $V'(\bar{r}) = V'(\bar{C}_t)$. In Eq. (3b), V_C is the Coulomb potential between the deformed daughter and the spherical emitted particle. It is defined by $Z_1 Z_2 e^2 / \bar{r}$ where Z_α and Z_d are the atomic numbers of alpha and daughter nuclei. Also, in Eq. (3b), $V_\ell(\bar{r})$ by defining $\ell(\ell + 1)/2\mu\bar{r}^2$ depicts the centrifugal potential, l is the orbital angular momentum of the cluster nucleus and $\bar{r} = z + \bar{C}_d(\theta) + C_c$ is the distance between the fragment centers, and z is the distance between the near surfaces of the fragments. The touching configuration of two nuclei C_t is evaluated by averaging the C_t over the polar angle between the symmetry axes of axially symmetric deformed parent or daughter nuclei and the direction of alpha emission, i.e., \bar{C}_t is obtained by averaging $C_t(\theta)$ along the orientation θ [36],

$$\bar{C}_t = \frac{1}{2} \int_0^\pi C_t(\theta) \sin \theta d\theta, \quad (4)$$

and $C_t(\theta)$ is defined as

$$C_t(\theta) = C_d(\theta) + C_c, \quad (5)$$

where C_c and $C_d(\theta)$ are the Sussmann central radius of the EC and daughter respectively. C_c refers to the sharp radii (R_c) as

$$C_c = R_c - b^2/R_c, \quad (6)$$

and $C_d(\theta)$ is related to $R_d(\theta)$ via [36]

$$C_d(\theta) = R_d(\theta) - \frac{1}{2} k b^2, \quad (7)$$

where k is the total curvature of the surface at the point under consideration. \bar{R}_d is obtained by averaging $R_d(\theta)$ along the orientation θ as

$$\bar{R}_d = \frac{1}{2} \int_0^\pi R_d(\theta) \sin \theta d\theta. \quad (8)$$

In the above expressions, the total curvature of the surface at the point under consideration is defined as

$$k = \frac{1}{R_\theta} + \frac{1}{R_\phi}, \quad (9)$$

where R_θ and R_ϕ , the two principal radii of curvature of the surface, are defined as [36]

$$R_\theta(\theta) = \frac{R u(\theta)^3}{\lambda w(\theta)}, \quad (10a)$$

$$R_\phi(\theta) = \frac{R u(\theta)}{\lambda} \frac{\beta_1 + \beta_2 \cos^3 \theta + \beta_3 \cos^4 \theta}{\beta_1 + 3\beta_2 \cos^3 \theta + 5\beta_3 \cos^4 \theta}; \quad (10b)$$

also in Eq. (10a), $u(\theta)$ and $w(\theta)$ are expressed as follows:

$$u(\theta) = [\beta_1^2 + 2\beta_2(\beta_1 + 2\beta_2)\cos^2 \theta + (2\beta_1\beta_3 + 16\beta_2\beta_3 - 3\beta_2^2\cos^4 \theta + 2\beta_3(8\beta_3 - 7\beta_2)\cos^6 \theta - 15\beta_3^2\cos^8 \theta)^{1/2}], \quad (11)$$

and

$$w(\theta) = (\beta_1^2 - 2\beta_1\beta_2) + 6(\beta_1\beta_2 + \beta_2^2 - 2\beta_1\beta_3)\cos^2 \theta + 3(6\beta_1\beta_3 + 6\beta_2\beta_3 - \beta_2^2)\cos^4 \theta + 10\beta_3(2\beta_3 - \beta_2) \times \cos^6 \theta - 15\beta_3^2\cos^8 \theta, \quad (12)$$

where β_1, β_2 , and β_3 parameters are

$$\begin{aligned} \beta_1 &= 1 - \frac{1}{2}\alpha_2 + \frac{3}{8}\alpha_4, \\ \beta_2 &= \frac{3}{2}\alpha_2 - \frac{15}{4}\alpha_4, \\ \beta_3 &= \frac{35}{8}\alpha_4. \end{aligned} \quad (13)$$

The deformation parameter $\beta_1 = \beta_{10}$ is determined via [37]

$$\beta_{lm} = \sqrt{4\pi} \frac{\int R_i(\theta, \varphi) Y_l^m(\theta, \varphi) d\Omega}{\int R_i(\theta, \varphi) Y_0^0(\theta, \varphi) d\Omega}, \quad (14)$$

TABLE I. Comparison of considered values of the logarithm of half-life time for the case with parent and daughter deformation with experimental values [48,49] and with the values of UNIV and UDL. The deformation β_2 and β_4 are taken from [47].

PN	DN	EC	π_p	π_d	ℓ_{\min}	Q_c (MeV)	Deformation			$\log_{10}(T_{1/2})$			
							P		D	Expt.	Present work	UDL	UNIV
							β_2	β_4	β_2				
^{221}Fr	^{207}Tl	^{14}C	5/2-	$1/2+$	3	31.28	0.098	-0.060	0.003	14.52	15.22	15.83	14.24
^{221}Ra	^{207}Pb		5/2+	$1/2-$	3	31.39	0.098	-0.060	0.003	13.39	13.41	16.68	14.92
					2						13.32		
^{222}Ra	^{208}Pb		0+	0+	0	32.40	0.104	-0.060	0.003	11.01	11.05	14.48	13.06
^{223}Ra	^{209}Pb		3/2+	9/2+	4	30.62	0.138	-0.075	0.003	15.04	15.10	18.30	16.29
^{224}Ra	^{210}Pb		0+	0+	0	30.53	0.144	-0.075	0.003	15.68	14.95	18.46	16.42
^{225}Ac	^{211}Bi		3/2-	9/2-	4	30.48	0.151	-0.080	0.003	17.16	16.41	19.65	17.39
^{226}Ra	^{212}Pb		0+	0+	0	28.21	0.151	-0.080	0.003	21.34	20.30	23.98	21.17
^{228}Th	^{208}Pb	^{20}O	0+	0+	0	44.72	0.182	0.112	0	20.72	19.01	23.56	21.90
^{230}U	^{208}Pb	^{22}Ne	0+	0+	0	61.40	0.199	0.115	0	19.57	19.33	21.38	20.18
^{230}Th	^{206}Hg	^{24}Ne	0+	0+	0	56.20	0.185	-0.075	-0.003	24.61	24.59	28.76	26.99
^{231}Pa	^{207}Tl		3/2-	$1/2+$	2	58.15	0.185	-0.080	0.003	22.88	22.65	26.71	25.30
^{232}U	^{208}Pb		0+	0+	0	60.26	0.192	-0.080	0.003	20.40	20.47	24.48	23.48
^{233}U	^{209}Pb		5/2+	9/2+	2	57.85	0.192	-0.080	0.003	24.84	24.63	28.76	26.87
					0						24.58		
^{234}U	^{210}Pb		0+	0+	0	57.09	0.198	-0.075	0.003	25.92	25.87	30.12	27.95
^{233}U	^{208}Pb	^{25}Ne	5/2+	0+	0	58.01	0.207	0.117	0	24.82	24.63	29.17	27.63
^{232}Th	^{206}Hg	^{26}Ne	0+	0+	0	59.52	0.192	-0.070	-0.003	>29.20	29.81	23.76	23.93
^{234}U	^{208}Pb		0+	0+	0	62.21	0.196	-0.075	0.003	25.88	25.79	22.11	22.55
^{234}U	^{206}Hg	^{28}Mg	0+	0+	0	70.52	0.198	-0.075	-0.003	27.54	27.47	31.07	29.79
^{236}Pu	^{208}Pb		0+	0+	0	76.42				21.67	21.57	24.80	24.88
^{238}Pu	^{210}Pb		0+	0+	0	73.72	0.205	-0.060	0.003	25.70	25.57	29.00	28.07
^{237}Np	^{207}Tl	^{30}Mg	5/2+	$1/2+$	2	72.11	0.198	-0.070	0.003	>26.90	26.98	31.07	30.65
^{238}Pu	^{208}Pb		0+	0+	0	74.04	0.025	-0.060	0.003	25.70	25.51	29.54	29.42
^{238}Pu	^{206}Hg	^{32}Si	0+	0+	0	88.41	0.205	-0.060	-0.003	25.27	25.22	27.75	28.53
^{241}Am	^{207}Tl	^{34}Si	5/2-	$1/2+$	3	89.41	0.212	-0.050	0.003	>25.30	25.83	28.77	30.21
			0								25.76		
^{242}Cm	^{208}Pb		0+	0+	0	92.44	0.224	0.079	0	23.15	23.22	26.06	28.18

where $Y_{lm}(\theta, \varphi)$ denotes the spherical harmonics and is given by [37]

$$Y_{lm}(\theta, \varphi) \equiv (-1)^m \sqrt{\frac{2l+1}{4\pi} \frac{(l-m)!}{(l+m)!}} P_l^m(\cos\theta) e^{im\varphi}. \quad (15)$$

The radii of the deformed nuclei are considered as [38]

$$R_i(\theta) = R_{i0} \left[1 + \sum_{n=0}^{\infty} \alpha_n P_n[\cos(\theta)] \right], \quad (16)$$

where $i = 0, 1, 2$, respectively, denote the parent, daughter, and the alpha particle and $\alpha_l = \sqrt{2l+1}/4\pi \beta_l$ is the deformation parameter. The proximity potential V_p is given by Blocki

et al. [39] as

$$V_{\text{prox}}(z) = 4\pi\gamma b \left(\frac{\bar{C}_d C_\alpha}{\bar{C}_t} \right) \Phi \left(\frac{r - \bar{C}_d - C_\alpha}{b} \right), \quad (17)$$

where $\varepsilon = z/b = (r - \bar{C}_t)/b$. The nuclear surface tension coefficient for this potential is defined by [39] $\gamma = \gamma_0 [1 - k_s I^2] (\text{MeV}/\text{fm}^2)$, where γ (MeV/fm^2) is called the surface energy constant in the Lysekil mass formula. This potential is related to Prox 1977 [39], $\gamma = 0.9517 [1 - 1.7826(N-Z/A)^2]$, with $\gamma_0 = 0.9517 \text{ MeV}/\text{fm}^2$ and $k_s = 1.7826$. The universal proximity potential was obtained from the Thomas-Fermi

model with the inclusion of a momentum dependent nucleon-nucleon interaction potential, and is given by [40]

$$\Phi_1(\varepsilon) = -1.7817 + 0.9270\varepsilon + 0.0169\varepsilon^2 - 0.05148\varepsilon^3, \quad \text{for } 0 \leq \varepsilon \leq 1.9475, \quad (18a)$$

$$\Phi_2(\varepsilon) = -4.41 \exp(-\varepsilon/0.7176), \quad \text{for } \varepsilon \geq 1.9475. \quad (18b)$$

The results are listed in Table I. The resulting potential barriers for the cluster ^{14}C emission of ^{223}Ra with decay equation $^{223}\text{Ra} \rightarrow ^{14}\text{C} + ^{209}\text{Pb}$ ($Q = 30.62$ MeV) are displayed in Fig. 1

III. COMPARISON WITH THE SEMIEMPIRICAL FORMULA

In the past few decades, several efforts were made to develop theoretical and semiempirical formulas for the estimation of the α -decay and cluster radioactivity half-lives. It is well known that the majority all the defined formulas depend on the mass number of the parent and cluster emitter (A_p , A_c), the charge number of the parent and cluster emitter (Z_p , Z_c), and the released energy of the EC (Q_c). Also, the authors strived to define the modifiable parameters of these equations by fitting them into the available experimental cluster radioactivity and α -decay half-lives.

A. UNIVERSAL DECAY LAW OF QI

A linear universal decay formula started from the microscopic mechanism of the charged particle emission and the α -like (extension to the heavier cluster of α -decay theory) R -matrix theory for all kinds of clusters and isotopic modes defined by Qi *et al.* [41], and it is entitled the universal decay law (UDL). The UDL formula holds for the monopole radioactive decay of all clusters and depends only on the mass,

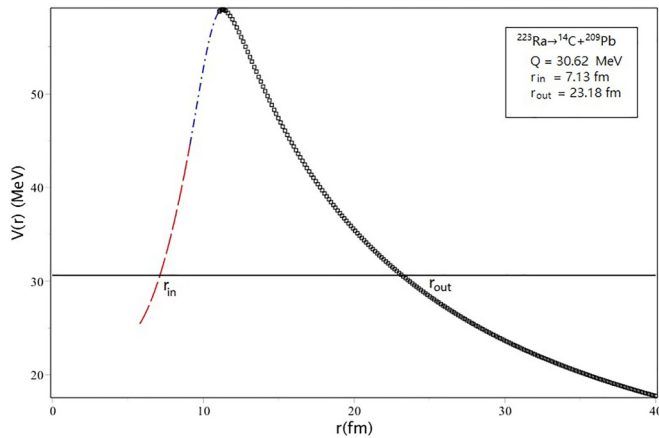


FIG. 1. Potential barrier including a nuclear proximity energy term corrections vs emission of ^{14}C from the ^{223}Ra mother nucleus vs the distance between the mass centers [r (fm)] for $^{223}\text{Ra} \rightarrow ^{14}\text{C} + ^{209}\text{Pb}$ with $Q = 30.62$ MeV. $R_{\text{in}} = 7.13$ (fm) and $R_{\text{out}} = 23.18$ (fm) are the inner and outer turning points. We consider three parts for the potential barrier; $a \leq r \leq c_t$, this is an overlapping region where a is the first turning point, c (fm) is the touching configuration, $c_t \leq r \leq c$ and $c \leq r \leq b$, and b is the second turning point.

atomic numbers of the parent nuclei and EC, and the Q value. The UDL formula thus obtained is given as

$$\log_{10} T_{1/2} = a Z_C Z_d \sqrt{\frac{A}{Q_C}} + b \sqrt{A Z_C Z_d (A_d^{1/3} + A_C^{1/3})} + c$$

$$= a \chi' + b \rho' + c, \quad (19)$$

where $A = A_d A_C / (A_d + A_C)$, A_d and A_C are the mass number of daughter and cluster emitter respectively. Q_C is the kinetic energy of cluster decay. The constants $a = 0.4314$ (the constant a is a free parameter that takes into account the effect of higher order terms of the Coulomb penetrability), $b = -0.4087$, and $c = -25.7725$ are the coefficient sets of Eq. (19). They are determined by fitting to the available experimental data, and the term $b \rho' + c$ defines the clusterization in the parent nucleus [42]. Equation (19) includes the Geiger-Nuttall Law (GNL) [42] as a special case, given as

$$\chi' = Z_d Z_\alpha \sqrt{\frac{A}{Q}} \quad (20)$$

and

$$\rho' = \sqrt{\frac{A_d A_\alpha}{(A_d + A_\alpha)}} Z_d Z_\alpha (A_d^{1/3} + A_\alpha^{1/3}) \quad (21)$$

B. UNIVERSAL CURVE (UNIV) OF POENARU ET AL.

Poenaru *et al.* [43] presented the estimation of the half-lives against the decay of transuranium nuclei including superheavies by three methods: a semiempirical formula taking into account the magic numbers of nucleons, the analytical supersymmetric fission model, and the universal curves. The universal (UNIV) curves, resulting from the development of a fission theory to larger mass asymmetry, should be named, among them, with major importance [44–46]. Based on the quantum mechanical tunneling procedure, in UNIV, the partial decay half-life T of the parent nucleus is defined as

$$T = \frac{\ln 2}{\lambda} = \frac{\ln 2}{\nu S P_s}, \quad (22)$$

where three model-dependent quantities are $\nu = 10^{22.01} \text{ s}^{-1}$, S (according to Poenaru and Greiner's work [45], $S_\alpha = 0.0143153$), and P_s is the frequency of assaults on the barrier per second, the preformation probability of the cluster at the nuclear surface that S depends only on the mass number of the EC, A_e (equal to the penetrability of the internal part of the barrier in a fission theory), and the quantum penetrability of the external potential barrier by fitting to the available experimental data for α decay, the corresponding numerical values [44], respectively. By using the decimal logarithm,

$$\log_{10} T(s) = -\log_{10} P + \log_{10} S + [\log_{10}(\ln 2) - \log_{10} \nu]. \quad (23)$$

The decimal logarithm of the preformation factor is given by

$$\log_{10}S = -0.598(A_e - 1)_s, \quad (24)$$

and the additive constant for an even-even ($e-e$) nucleus is given as

$$c_{ee} = [-\log_{10}\nu + \log_{10}(\ln 2)] = -22.16917, \quad (25)$$

For even-odd ($e-o$), odd-even ($o-e$), and odd-odd ($o-o$) nuclei, we change c_{ee} by

$$\begin{aligned} c_{eo} &= c_{ee} + h_{eo}, \\ c_{oe} &= c_{ee} + h_{oe}, \\ c_{oo} &= c_{ee} + h_{oo}, \end{aligned} \quad (26)$$

where $h_{oe} = 0.445$, $h_{eo} = 0.294$, and $h_{oo} = 0.842$ are the mean values of the hindrance factors in these groups of nuclides for even-odd, odd-even, and odd-odd nuclei, respectively. The penetrability of an external Coulomb barrier, having separate distance at the touching configuration, i.e., the first turning point $R_a = R_t = R_d + R_e$, may be found systematically as

$$\begin{aligned} -\log_{10}P_s &= 0.22873(\mu_A Z_d Z_e R_b)^{1/2} \\ &\times \{\arccos \sqrt{r} - \sqrt{r(1-r)}\}, \end{aligned} \quad (27)$$

where $r = R_t/R_b$, $R_t = 1.2249(A_d^{1/3} + A_C^{1/3})$ and $R_b = 1.43998Z_d Z_C/Q$ and the liquid-drop-model radius constant $r_0 = 1.2249$ fm.

IV. DISCUSSION AND RESULTS

In this paper, we have studied the influence of the deformation of the daughter and parent nuclei on half-lives in exotic cluster decay. The effect of quadrupole (β_2) and hexadecapole (β_4) deformations of parent and fragments on half-life times are also calculated. It is significant to investigate the role of deformation parameters of nuclei and cluster decaying fragments because both the daughter and parent nuclei are deformed, and there is a motivation behind the introduction of the effect of the deformation of nuclei. Deformations depict their effect principally for the heavy and super heavy mass fragments. Therefore, the deformation influences are of importance for considering exotic cluster decays. The CR properties for different modes of exotic decay have been studied by evaluating the decay half-lives using the CPPMDN and the numerical results for C, O, Ne, Mg, and Si cluster radioactivity are given in Table I. The first six columns of Table I identify, respectively, the parent (PN) and daughter nuclei (DN), EC, and the ground-state spin and parity of them (π_p , π_d), in addition to the considered value of minimum angular momentum which was carried out by the emitted particle ℓ_{\min} . The seventh column denotes the values of the released energy (Q value) in MeV. The quadrupole (β_2) and hexadecapole (β_4) deformation components [47] of the deformed parent nuclei and the quadrupole (β_2) [47] of the deformed daughter nuclei as used in the calculations are summarized in Table I. The cluster half-life calculations have also been done using the universal decay law (UDL) of Qi

et al. [41] and the universal curve (UNIV) of Poenaru *et al.* [43]. The logarithms of the experimental half-lives (taken from the review of Refs. [48,49]) and the results from the CPPMDN, UNIV, and UDL models are also listed in the last column of Table I for comparison. A further comparison of CPPMDN with these two theoretical models shows that our data match these theoretical model calculations well. These evaluations and the comparisons have also been comprehended in Table I and we see that on comparison with the experimental cluster half-lives, it can be found that the half-lives estimated using CPPMDN are in good agreement with the experimental data. A model for studying exotic cluster radioactivity was developed by Silisteanu and Scheid [50] in 1995 so that one can study the main behaviors of clustering and penetration phenomena in nuclear many-particle systems. In 2003, Balasubramaniam *et al.* [49] proposed a new formula, a model-independent three parameter formula, as the semiempirical AZ formula (SemAZF), for cluster decay half-lives of nuclei and calculated the logarithms of decay half-lives of different ECs from various radioactive nuclei. In 2008, Ni *et al.* [51] presented a general formula (NRDX) of half-lives and decay energies for α decay and cluster radioactivity based on the WKB barrier penetration probability with some approximations. For comparison, in the last column of Table II the logarithms of the experimental half-lives [48,49] and the logarithms of the work of Balasubramaniam *et al.* [49] (SemAZF), Silisteanu and Scheid [50], and Ni *et al.* [51] (NRDX) are listed. In order to study the agreement between the experimental and calculated data, we have estimated the standard deviation σ for the half-lives. For the estimation of σ , we have calculated a total of 25 transitions as experimental data which are available only for these decays. Now we can obtain the standard deviation,

$$\sqrt{\langle \sigma^2 \rangle} = \sqrt{\sum_{i=1}^N [\log_{10}(T_{\text{exp}}^i / T_{\text{cal.}}^i)]^2 / N} \quad (28)$$

and the mean deviation is given by

$$\langle \sigma \rangle = \sum_{i=1}^N |\log_{10}(T_{\text{exp}}^i / T_{\text{cal.}}^i)| / N. \quad (29)$$

In Table III, the first column denotes the results of Refs. [41], [43], and [49–52]. The second column denotes the number of nuclei for all the nuclei groups. The standard deviations are listed in the fourth column of Table III.

The standard deviation of the logarithm of the half-life value is found to be 0.519 for CPPMDN, 0.537 for Silisteanu and Scheid [50], 0.560 for PGG [52] for the $e-e$ group, 0.655 for PGG [52] for an $o-e$ group, 0.734 for NRDX [51], 0.848 for PGG [52] for an $e-o$ group, 1.034 for the semiempirical AZ formula (SemAZF) [49], 2.832 for UNIV (universal curve [43]), and that for UDL (universal decay law [41]) is found to be 3.556. Among the several models, the standard deviation is least for CPPMDN. The next-lowest data of standard deviation can be seen for Silisteanu and Scheid's work [50], which is attributed to the addition of the parameters of resonance scattering effects, and PGG [52] for the $e-e$ group respectively. Therefore, it could be mentioned that

TABLE II. The comparison of the calculated CR half-lives with experimental values and with the values of SemAZF, NRDX, and Silisteanu and Scheid.

Mode of cluster radioactivity	Q_c (MeV)	$\log_{10}(T_{1/2})$			
		Expt.	SemAZF [49]	Silisteanu and Scheid [50]	NRDX [51]
$^{221}\text{Fr} \rightarrow ^{207}\text{Tl} + ^{14}\text{C}$	31.28	14.52	14.54	14.68	14.63
$^{221}\text{Ra} \rightarrow ^{207}\text{Pb} + ^{14}\text{C}$	31.39	13.39	12.96	12.39	13.47
$^{222}\text{Ra} \rightarrow ^{208}\text{Pb} + ^{14}\text{C}$	32.40	11.01	11.98	10.91	11.02
$^{223}\text{Ra} \rightarrow ^{209}\text{Pb} + ^{14}\text{C}$	30.62	15.04	13.81	15.85	14.54
$^{224}\text{Ra} \rightarrow ^{210}\text{Pb} + ^{14}\text{C}$	30.53	15.68	15.94	16.27	15.87
$^{225}\text{Ac} \rightarrow ^{211}\text{Bi} + ^{14}\text{C}$	30.48	17.16	16.20	17.33	18.23
$^{226}\text{Ra} \rightarrow ^{212}\text{Pb} + ^{14}\text{C}$	28.21	21.34	20.08	21.20	20.91
$^{228}\text{Th} \rightarrow ^{208}\text{Pb} + ^{20}\text{O}$	44.72	20.72	21.90		21.53
$^{230}\text{U} \rightarrow ^{208}\text{Pb} + ^{22}\text{Ne}$	61.40	19.57	21.78		20.09
$^{230}\text{Th} \rightarrow ^{206}\text{Hg} + ^{24}\text{Ne}$	56.20	24.61	25.77	24.89	24.57
$^{231}\text{Pa} \rightarrow ^{207}\text{Tl} + ^{24}\text{Ne}$	58.15	22.88	23.62	22.48	23.09
$^{232}\text{U} \rightarrow ^{208}\text{Pb} + ^{24}\text{Ne}$	60.26	20.40	22.24	20.44	20.36
$^{233}\text{U} \rightarrow ^{209}\text{Pb} + ^{24}\text{Ne}$	57.85	24.84	23.87	24.52	24.41
$^{234}\text{U} \rightarrow ^{210}\text{Pb} + ^{24}\text{Ne}$	57.09	25.92	25.42	25.86	
$^{233}\text{U} \rightarrow ^{208}\text{Pb} + ^{25}\text{Ne}$	58.01	24.82	24.15	24.41	
$^{232}\text{Th} \rightarrow ^{206}\text{Hg} + ^{26}\text{Ne}$	59.52	>29.20		29.07	
$^{234}\text{U} \rightarrow ^{208}\text{Pb} + ^{26}\text{Ne}$	62.21	25.88	25.85	25.77	
$^{234}\text{U} \rightarrow ^{206}\text{Hg} + ^{28}\text{Mg}$	70.52	27.54	26.24	26.16	25.24
$^{236}\text{Pu} \rightarrow ^{208}\text{Pb} + ^{28}\text{Mg}$	76.42	21.67	23.01		20.75
$^{238}\text{Pu} \rightarrow ^{210}\text{Pb} + ^{28}\text{Mg}$	73.72	25.70	25.70	26.51	
$^{237}\text{Np} \rightarrow ^{207}\text{Tl} + ^{30}\text{Mg}$	72.11	>26.90		27.19	
$^{238}\text{Pu} \rightarrow ^{208}\text{Pb} + ^{30}\text{Mg}$	74.04	25.70	25.71	25.87	
$^{238}\text{Pu} \rightarrow ^{206}\text{Hg} + ^{32}\text{Si}$	88.41	25.27	25.99	26.02	25.57
$^{241}\text{Am} \rightarrow ^{207}\text{Tl} + ^{34}\text{Si}$	89.41	>25.30		25.75	
$^{242}\text{Cm} \rightarrow ^{208}\text{Pb} + ^{34}\text{Si}$	92.44	23.15			23.51

the adequacy of the CPPMDN has been confirmed through the comparison of the present rms with those of previous works (which incorporated explicitly the deformation effect) as declared in Table III. Fig. 2 represents the comparison

between the logarithms of decay half-lives for different ECs from various radioactive parents, estimated by using CPPMDN, UNIV, UDL, and the available experimental values for $^{222}\text{Ra} \rightarrow ^{14}\text{C} + ^{208}\text{Pb}$ decay. We see that the ^{14}C emission

TABLE III. Comparison of the present RMS with other references.

Ref.	n C emitters	Group	σ
Present work	25 ($87 \leq Z \leq 96$)	all	0.519
Silisteanu and Scheid [50]	21	all	0.537
PGG (new universal plot [52])	(16 clusters)	$e-e$	0.560
	6	$e-o$	0.848
	5	$o-e$	0.665
NRDX [51]	17	all	0.734
Semiempirical AZ formula (SemAZF) [49]	21	all	1.034
UNIV (universal curve [43])	25	all	2.832
UDL (universal decay law [41])	25	all	3.556

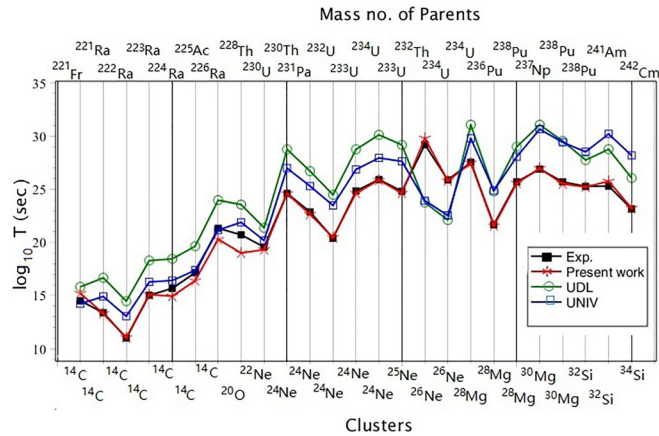


FIG. 2. The logarithms of decay half-lives for different EC from various radioactive parents, estimated by using CPPMDN, UNIV, and UDL and compared with the available experimental values (Exp.). The x axis is in terms of the mass number of the parent nuclei and the corresponding EC by these parents is labeled at the bottom x axis.

from ^{222}Ra and the ^{14}C emission from ^{221}Ra have the lowest half-lives among all the cluster emissions. The shortest half-life in Fig. 3 ($\log_{10}T_{1/2} = 11.05$ s) corresponds to the ^{14}C emission from ^{222}Ra ($^{222}\text{Ra} \rightarrow ^{208}\text{Pb} + ^{14}\text{C}$). In Fig. 3 we see that the values for the logarithm of the half-lives ($\log_{10}T_{1/2}$) plotted vs the decay energy ($Q^{-1/2}$), approximately lie on a straight line for all of the different parent nuclei between ^{221}Fr and ^{242}Cm emitting the clusters ^{14}C , ^{20}O , $^{22, 24, 25, 26}\text{Ne}$, $^{28, 30}\text{Mg}$, and $^{32, 34}\text{Si}$. We observed that this behavior is the same as the Geiger-Nuttall systematic behavior that is well known for the alpha half-lives.

V. CONCLUSION

In summary, the half-life of the decay of radioactive nuclei which emit heavy clusters such as C, O, Ne, Mg, and Si have been studied using the CPPMDN. The CR half-lives are also calculated using the universal decay law (UDL) of Qi *et al.*,

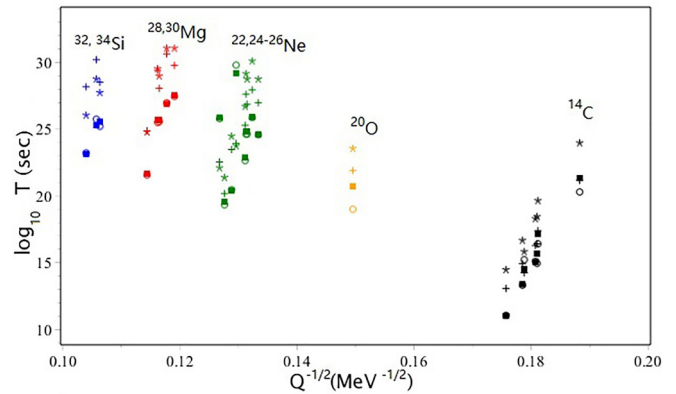


FIG. 3. Estimated and experimental half-lives [$\log_{10}T$ (sec) values] of cluster radioactivity as a function of $Q^{-1/2}$ in a Geiger-Nuttall plot and the plot for the cluster emission of ^{14}C from ^{221}Fr , $^{221-226}\text{Ra}$, and ^{225}Ac (black), ^{20}O from ^{228}Th (yellow), $^{22, 23-26}\text{Ne}$ from ^{230}U , ^{230}Th , ^{231}Pa , and $^{232-234}\text{U}$ (green), $^{28, 30}\text{Mg}$ from ^{234}U , $^{236, 238}\text{Pu}$, ^{237}Np , and ^{238}Pu (red), and $^{32, 34}\text{Si}$ from ^{238}Pu , ^{241}Am , and ^{242}Cm (blue). Also, filled squares show experimental data.

and the universal curve (UNIV) for cluster decay of Poenaru *et al.* The results thus obtained were compared with the corresponding experimental data and the models, the semiempirical AZ formula (SemAZF), Silisteanu and Scheid work, and the new universal plot of Poenaru *et al.*, and it is found that they match well over an extensive range. Also, the outcomes depict excellent agreement between the experimental data and the calculated values. When deformation effects are included, half-life values are found to be decreased, even though it is small. We hope that these predictions will be a guide for future experimental research on CR phenomena.

ACKNOWLEDGMENTS

The authors take great pleasure in thanking the referee for his/her several suggestions and comments. This research was supported by a research grant of the University of Mazandaran, Under Contract of Research Project No. 76374.

- [1] A. Sandulescu, D. N. Poenaru, and W. Greiner, *Sov. J. Part. Nucl.* **11**, 528 (1980).
- [2] H. J. Rose and G. A. Jones, *Nature (London)* **307**, 245 (1984).
- [3] D. N. Poenaru, M. Ivascu, A. Sandulescu, and W. Greiner, *Phys. Rev. C* **32**, 572 (1985).
- [4] D. N. Poenaru, R. A. Gherghescu, and W. Greiner, *Phys. Rev. Lett.* **107**, 062503 (2011).
- [5] D. N. Basu, *Phys. Rev. C* **66**, 027601 (2002).
- [6] R. K. Sheline and I. Ragnarsson, *Phys. Rev. C* **55**, 732 (1997).
- [7] C. Xu and Z. Ren, *Phys. Rev. C* **69**, 024614 (2004).
- [8] S. Kumar and R. K. Gupta, *Phys. Rev. C* **49**, 1922 (1994).
- [9] G. Shanmugam and B. Kamalaharan, *Phys. Rev. C* **41**, 1184 (1990).
- [10] P. N. Poenaru, R. A. Gherghescu, and W. Greiner, *Rom. J. Phys.* **58**, 1157 (2013).
- [11] R. K. Gupta and W. Greiner, *Int. J. Mod. Phys. (Suppl.)* **3**, 335 (1994).
- [12] S. K. Arun, R. K. Gupta, B. B. Singh, S. Kanwar, and M. K. Sharma, *Phys. Rev. C* **79**, 064616 (2009).
- [13] S. Kumar and R. K. Gupta, *Phys. Rev. C* **55**, 218 (1997).
- [14] D. N. Poenaru, W. Greiner, and M. Ivascu, *Nucl. Phys. A* **502**, 59 (1989).
- [15] S. P. Tretyakova, *Radiat. Meas.* **25**, 279 (1995).
- [16] H. F. Zhang, J. M. Dong, G. Royer, W. Zuo, and J. Q. Li, *Phys. Rev. C* **80**, 037307 (2009).
- [17] S. K. Arun, R. K. Gupta, S. Kanwar, B. B. Singh, and M. K. Sharma, *Phys. Rev. C* **80**, 034317 (2009).
- [18] Z. Ren, C. Xu, and Z. Wang, *Phys. Rev. C* **70**, 034304 (2004).
- [19] D. N. Poenaru, Y. Nagame, R. A. Gherghescu, and W. Greiner, *Phys. Rev. C* **65**, 054308 (2002).

- [20] B. Buck, C. B. Dover, and J. P. Vary, *Phys. Rev. C* **11**, 1803 (1975).
- [21] M. A. Souza and H. Miyake, *Braz. J. Phys.* **35**, 826 (2005).
- [22] M. A. Souza and H. Miyake, *Phys. Rev. C* **91**, 034320 (2015).
- [23] M. A. Souza and H. Miyake, *Eur. Phys. J. A* **53**, 146 (2017).
- [24] M. A. Souza and H. Miyake, *Phys. Rev. C* **104**, 064301 (2021).
- [25] M. A. Souza, H. Miyake, T. Borello-Lewin, C. A. da Rocha, and C. Frajuca, *Phys. Lett. B* **793**, 8 (2019).
- [26] B. Buck, A. C. Merchant, and S. M. Perez, *Phys. Rev. C* **51**, 559 (1995).
- [27] B. Buck, J. C. Johnston, A. C. Merchant, and S. M. Perez, *Phys. Rev. C* **52**, 1840 (1995).
- [28] B. Buck, A. C. Merchant, and S. M. Perez, *Phys. Rev. C* **61**, 014310 (1999).
- [29] F. Michel, G. Reidemeister, and S. Ohkubo, *Phys. Rev. C* **61**, 041601(R) (2000).
- [30] S. A. Gurvitz and G. Kalbermann, *Phys. Rev. Lett.* **59**, 262 (1987).
- [31] F. Hoyler, P. Mohr, and G. Staudt, *Phys. Rev. C* **50**, 2631 (1994).
- [32] B. Buck, J. C. Johnston, A. C. Merchant, and S. M. Perez, *Phys. Rev. C* **53**, 2841 (1996).
- [33] C. Xu and Z. Ren, *Phys. Rev. C* **68**, 034319 (2003).
- [34] E. Javadimanesh *et al.*, *Mod. Phys. Lett. A* **27**, 1250226 38, (2012).
- [35] H. Hassanabadi and S. S. Hosseini, *Nucl. Phys. A* **974**, 72 (2018).
- [36] Y. J. Shi and W. J. Swiatecki, *Nucl. Phys. A* **464**, 205 (1987).
- [37] P. Moller, J. R. Nix, W. D. Myers, and W. J. Swiatecki, *At. Data Nucl. Data Tables* **59**, 185 (1995).
- [38] H. J. Krappe, J. R. Nix, and A. J. Sierk, *Phys. Rev. C* **20**, 992 (1979).
- [39] J. Blocki, J. Randrup, W. J. Swiatecki, and C. F. Tsang, *Ann. Phys. (N.Y.)* **105**, 427 (1977).
- [40] J. Blocki and W. J. Swiatecki, *Ann. Phys. (N.Y.)* **132**, 53 (1981).
- [41] C. Qi, F. R. Xu, R. J. Liotta, and R. Wyss, *Phys. Rev. Lett* **103**, 072501 (2009).
- [42] H. Geiger and J. M. Nuttall, *Philos. Mag.* **22**, 613 (1911).
- [43] D. N. Poenaru, I. H. Plonski, and W. Greiner, *Phys. Rev. C* **74**, 014312 (2006).
- [44] D. N. Poenaru and W. Greiner, *J. Phys. G: Nucl. Part. Phys.* **17**, S443 (1991).
- [45] D. N. Poenaru and W. Greiner, *Phys. Scr.* **44**, 427 (1991).
- [46] D. N. Poenaru, I. H. Plonski, R. A. Gherghescu, and W. Greiner, *J. Phys. G: Nucl. Part. Phys.* **32**, 1223 (2006).
- [47] P. Moller and J. R. Nix, *Nucl. Phys. A* **361**, 117 (1981).
- [48] NuDat2.4, <http://www.nndc.bnl.gov> (last update July 15, 2008).
- [49] M. Balasubramaniam, S. Kumarasamy, N. Arunachalam, and R. K. Gupta, *Phys. Rev. C* **70**, 017301 12 (2004).
- [50] I. Silisteanu and W. Scheid, *Phys. Rev. C* **51**, 2023 (1995).
- [51] D. Ni, Z. Ren, T. Dong, and C. Xu, *Phys. Rev. C* **78**, 044310 (2008).
- [52] D. N. Poenaru, R. A. Gherghescu, and W. Greiner, *Phys. Rev. C* **83**, 014601 (2011).